Highlights of Vehicles

ISSN 2696-8347, A Peer-Reviewed Open Access Journal by Highlights of Science

https://www.hos.pub/ho/vehicles

Optimal Fast-charging Strategy for Cylindrical Li-ion Cells

by Joris Jaguemont, Ali Darwiche and Fanny Bardé

Cite this Article

Jaguemont, J., Darwiche, A., & Bardé, F. (2024). Optimal Fast-charging Strategy for Cylindrical Li-ion Cells. *Highlights of Vehicles*, *2*(2), 24–34. https://doi.org/10.54175/hveh2020003

Highlights of Science

Publisher of Peer-Reviewed Open Access Journals

https://www.hos.pub

Barcelona, Spain

Article

Optimal Fast-charging Strategy for Cylindrical Li-ion Cells

Joris Jaguemont *, **Ali Darwiche** and **Fanny Bardé**

SOLiTHOR, Ondernemeerslaan 5429, 3800 Sint-Truiden, Belgium
* For correspondence: joris.jaguemont@solithor.com

Abstract This paper presents an innovative approach to optimize the fast-charging strategy for cylindrical Li-ion NMC 3Ah cells, with a focus on enhancing both charging efficiency and thermal safety. Leveraging the power of Model Predictive Control (MPC), we introduce a cost function that approximates the thermal safety boundary of Li-ion batteries, revealing a relationship between temperature gradient and state of charge. Our proposed approach formulates the fast and safe charging problem as an optimal output regulator problem, incorporating thermal safety margin constraints. To solve the optimization problem, we develop an MPC algorithm. Our charge control structure incorporates an equivalent circuit model coupled with a thermal equation for battery state of charge and temperature estimation. Through numerical validation with real experimental data obtained from testing an NMC 3Ah cylindrical cell, we demonstrate that our approach respects the battery's electrical and thermal constraints throughout the charging process.

Keywords lithium; charging; modelling; MPC; thermal control

1. Introduction

Lithium-ion batteries (LiBs) have become an integral part of modern technology, finding applications in devices such as laptops, cell phones, and automobiles [1]. One pressing challenge in the battery industry revolves around the rapid charging of batteries while ensuring safety and minimizing degradation. Lengthy charging times stand as a significant obstacle to the widespread adoption of electric vehicles (EVs) [2]. To address this issue, the development of fast-charging stations is crucial [3]. These systems play a pivotal role in ensuring swift and dependable charging, ultimately maximizing the efficiency of batteries. However, there exists a delicate balance when it comes to charging at high C-rates, as it introduces inherent tradeoffs with battery thermal gradient and lifespan [4]. Elevated C-rates accelerate ageing due to factors such as increased temperatures, a heightened growth rate of the solid-electrolyte interface (SEI) layer, elevated lithium plating, and greater mechanical stresses [5–7].

Numerous offline optimal control algorithms have been proposed to mitigate the adverse effects of fast charging. These algorithms tackle real-time optimal charging problems, primarily employing constrained such as dynamic programming (DP) [8], Pontryagin's minimum principle (PMP) [9], and Model Predictive Control (MPC) [10–12]. Among these optimization methods, the MPC algorithm has recently emerged as a promising solution for online optimization problems [10–12]. Moreover, previous works have demonstrated various approaches to employing MPC for battery fast charging [13–15]. While these studies contribute significantly to the field, they often rely on complex models and lack comprehensive experimental validation under varying conditions.

Therefore, this paper presents an MPC-based fast-charging controller that integrates a simple yet high-fidelity electro-thermal model. This model accurately represents the cell's electrical and thermal behaviour and incorporates practical future information prediction. Unlike previous approaches, this study emphasizes a balance between thermal safety and state of charge (SoC) optimization under real-world conditions. The scenario is based on a fast-charging application, and after extensive testing on an NMC 3Ah cylindrical cell, the model's validation confirms its reliability for the optimization process. This simple approach provides a comprehensive solution for optimizing fast-charging strategies, ensuring safety, efficiency, and practical applicability.

This approach aims to fill the gap in the current research by providing a validated and practical solution for optimizing fast-charging strategies for Li-ion batteries. The tailored MPC system enhances thermal performance and minimizes charging time trade-offs, ensuring that the cell's

Received: 22 May 2024
Accepted: 27 August 2024
Published: 9 September 2024

Academic Editor
Abbas Fotouhi, Cranfield University, UK

temperature self-regulates within safe limits. This development holds the potential to downsize cooling systems, offering substantial cost, weight, and volume savings in battery pack design.

The structure of this paper is as follows: Section 2 details the experimental setup used for the fast-charging test, while Section 3 outlines the fast-charging results. Section 4 covers the development of the electro-thermal and MPC models. Section 5 presents the optimization results. Finally, the conclusions are provided in Section 6.

2. Experimental Setup

2.1. Battery Feature

The tested batteries were cylindrical VTC6 3Ah 18650-type LiBs with the Li(NiMnCo)1/3O2 cathode and carbon anode, and the average mass was measured to be 46.6 g. The nominal capacity and voltage of the battery were 3 Ah and 3.7 V, respectively. The Neware CT-4008 (25 mV to 5 V—0.5 mA to 6 A) controlled by the computer was used to cycle the LiBs with the standard charging and discharging current of A, according to the battery specification [16]. A type-K thermocouple was attached to the cell and used to monitor the battery temperature. Figure 1 depicts the fast-charging experimental setup.

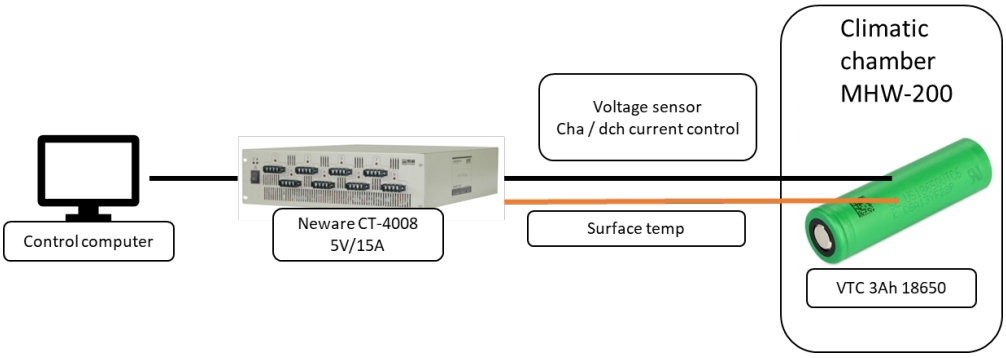

Figure 1. Schematic of the experimental setup used for testing the VTC6 NMC/G 3Ah.

2.2. Fast-charging Profile

The fast-charging profile comprises a high charging current of 4C (12 A) until the battery voltage reaches its maximum level of 4.2 V. This is followed by a constant voltage (CV) phase, continuing until the cut-off current reaches C/20 (0.15 A), where "C" represents the capacity of the cell. The fast-charging mission profile is designed to emulate a real-world fast-charging scenario involving the application of high currents [17–19]. To provide a more comprehensive overview, the testing procedure encompasses the following stages:

- Charging at C/3 from 0% to 10% SoC.
- Charging at 4C from 10% SoC up to the upper cut-off voltage of 4.2 V.
- Maintaining a CV phase until the charge rate reaches C/20.

For a visual representation of the fast-charging profile, please refer to Figure 2.

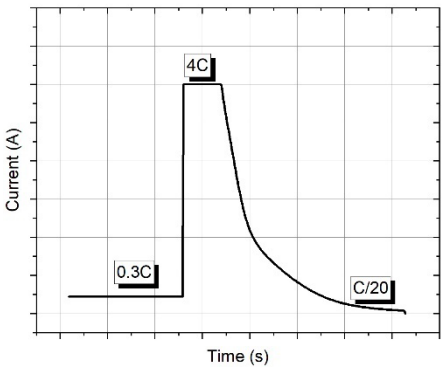

Figure 2. Fast-charging profile.

3. Fast-charging Results

In Figure 3, the results illustrate the fast-charging profile of a 3Ah NMC cell at 25 °C. The results, visualized concerning current, SoC, and temperature over time, reveal distinct characteristics. Initially, at a low current rate (C/3 or 1 A), the SoC gradually reaches 10% over 18 minutes. However, upon transitioning to the high current phase (4C or 12 A), characterized by rapid charging, the SoC swiftly surges to 80% in less than 15 minutes. These values represent current commercial targets and underscore the remarkable performance of these cells.

Regarding the temperature aspect, during the initial 0% to 10% SoC range, the cell's temperature remains relatively stable, owing to the low current rate. However, as the 4C (12 A) phase begins, the temperature escalates to 54 °C. These temperature levels raise pertinent concerns at the battery pack level, emphasizing the imperative need for meticulous charging strategies. Such strategies are indispensable to mitigate overheating risks, ensuring both the safety and long-term operational integrity of the battery pack.

In the end, achieving rapid charging of these cells necessitates a delicate equilibrium between maintaining desired SoC levels and managing temperature dynamics.

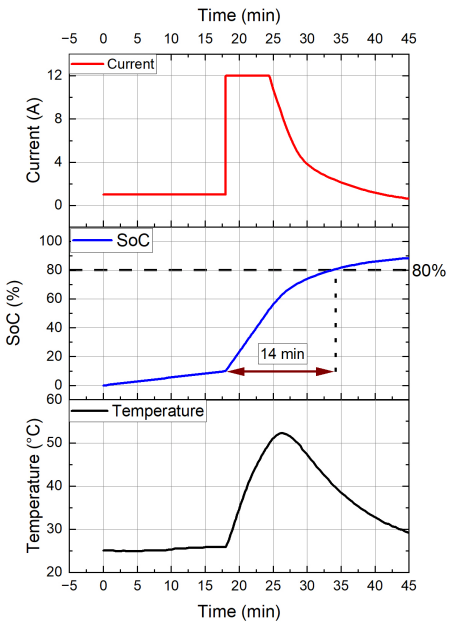

Figure 3. Fast-charging results of the NMC VTC6 3Ah cell.

4. Model Development

4.1. Model Methodology

This paper employs a 1D electro-thermal model based on a semi-empirical approach implemented within a MATLAB/Simulink® interface. The primary objective of this model is to replicate the electrical and thermal performance of the cell through two key components: the electrical and thermal modules. The first module focuses on calculating the SoC using electrical parameters, while the second module estimates the cell's temperature based on the heat generation equation.

The electrical model is constructed using the R_{int} model [20], as illustrated in Figure 4. It comprises a voltage source in series with a single resistance. In accordance with the equivalent circuit model, the battery's output voltage for the Li-ion cell is determined by the voltage drop resulting from factors such as the battery's open circuit voltage (OCV) and internal resistance (R_{int}). The output voltage of the cell is then calculated using the formula described in [20]:

$$V_{cell} = V_{oc} - R_{int} \cdot I_{batt} \tag{1}$$

where I_{batt} is the flowing current in the battery (A), Thereafter, the SoC is determined by the coulomb-counting method and is defined as [21]:

$$SoC = SoC_0 - \frac{1}{C_{init}} \int I_{batt} dt \tag{2}$$

with SoC_0 the initial SoC of the cell. C_{init} is defined as the initial capacity (Ah) and it is assumed to be temperature-dependent as well as influenced by the current. In Equation (1), all the circuit parameters are derived from the manufacturer's datasheet, resulting in an internal resistance value of 28 mΩ.

The thermal aspect of the model addresses the thermodynamic equations applicable to cylindrical-shaped cells. In this section, a single temperature point is considered. This implies that heat is generated at a specific location on the cell's surface, characterized by a particular heat capacity and mass. Subsequently, this heat is transferred from the cell's surface to the surrounding environment. By performing a heat balance equation at this specific point on the surface, we derive the following equations from thermodynamics, which describe the heat transfer between the surface and the ambient [22]:

$$\left\{ \begin{array}{c} \frac{dU_{cell}}{dt} = Q_{gen}(t) - Q_{loss}\,(t) = m.\,C_p.\frac{dT}{dt} \\ Q_{gen} = R_{int}.\,(I_{batt})^2 \\ Q_{loss} = Q_{conv} = h_{conv}.\,S_{area}.\,(T_{cell} - T_{amb}) \end{array} \right\} \tag{3}$$

where U_{cell}, the internal energy, is the total energy contained by a thermodynamic system (J), Q_{gen} is the generating heating rate (W) in the corresponding element, Q_{loss} is the heat losses of the corresponding element (W), C_p is the specific heat of the cell (kJ/kg.K), and *m* is the mass of the cell (kg). The thermal model operates under the following assumptions:

- The temperature of the cell's surface, denoted as T_{cell}, is considered to be uniformly distributed, and as such, it represents the overall temperature of the entire cell.
- This paper accounts for natural convective heat transfer, characterized by the following parameters: ambient temperature, T_{amb} (°C), the heat exchange surface area, S_{area} (in m^2), and the convective heat transfer coefficient, h_{conv} (W/m^2.K).

The thermal parameters are crucial for the model's accuracy as they directly influence the predicted temperature profile of the cell under various operating conditions. The careful selection of these values from the manufacturer's datasheet ensures that the model remains faithful to the actual physical behaviour of the battery. These parameters include:

- Specific Heat Capacity (C_p): This value indicates the amount of heat required to raise the temperature of the cell by one degree Kelvin. The chosen specific heat capacity of 1006 kJ/kg.K reflects the material properties of the cell, ensuring accurate thermal modelling.
- Mass (*m*): The mass of 0.046 kg is derived from the actual cell specifications, providing a realistic basis for thermal calculations.
- Surface Area (S_{area}): The area of 0.004327 m^2 corresponds to the surface area available for heat exchange, which is critical for determining the rate of convective heat transfer.
- Convective Heat Transfer Coefficient (h_{conv}): A value of 15 W/m^2.K is chosen based on typical natural convection conditions, ensuring that the model realistically captures the cooling effects in a natural environment.

All thermal parameters utilized in this paper are sourced from the cell manufacturer's datasheet. Consequently, the model employs a specific heat capacity (C_p) of 1006 kJ/kg.K, a mass of 0.046 kg, and an area of 0.004327 m^2 are used. Given the use of natural convection, an h_{conv} of 15 W/m^2.K is applied [23].

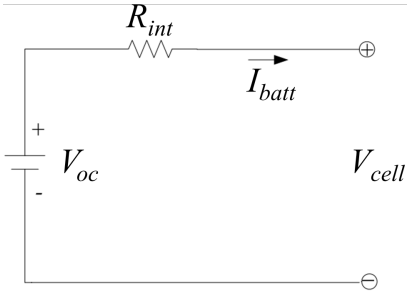

Figure 4. The R_{int} electrical model [20].

4.2. Model Validation

The results of model validation are presented in Figure 5, which displays the comparison between the measured and estimated SoC and temperature for the cell during the fast-charging phase (4C or 12 A). Table 1 lists the model deviation for which an average of 1% error. The model deviation is calculated with the root-mean-square error (RMSE) and showcases the deviation from the measurement data. A close examination of the figures reveals that the modelled SoC closely aligns with the SoC derived from the electrical experiments. This alignment serves as further substantiation of the electrical modelling and the accuracy of the electrical parameters.

Furthermore, in terms of temperature evolution, the model, despite employing only a single resistance, demonstrates remarkable accuracy in predicting the cell's temperature for which a minor model deviation has been found. Consequently, the strong agreement between the model's predictions and the experimental results for both electrical and thermal behaviours underscores the model's validity. Therefore, the electro-thermal model stands as a reliable tool for optimization processes.

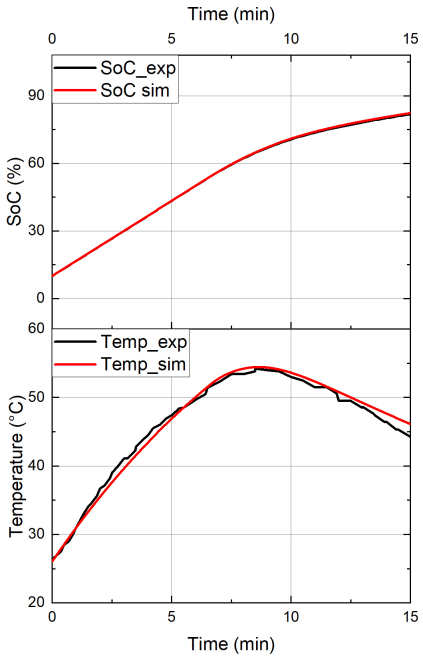

Figure 5. Validation of the electrical and thermal model.

Table 1. Electro-thermal model deviation.

Parameters	RMSE (%)
SoC (%)	0.6
Temperature (°C)	1.8

4.3. MPC

MPC is a sophisticated control strategy employed in various fields, including engineering, economics, and robotics [24,25]. At its core, MPC is a dynamic optimization technique that utilizes a mathematical model of a system to make control decisions. Unlike traditional control methods, MPC operates over a defined prediction horizon, which is a time window into the future. During this horizon, the controller predicts how the system will respond to various control inputs. Figure 6 shows the flowchart of the MPC and the semi-empirical model.

Moreover, MPC formulates an optimization problem that seeks to optimize a cost or objective function over the prediction horizon. The objective function typically includes terms related to system performance, such as tracking a reference trajectory or minimizing a cost, while considering constraints. At each time step, MPC solves the optimization problem based on the current state of the system and the prediction horizon. It calculates the optimal control inputs over the horizon but only applies the first input to the system. After applying the first control input, MPC advances to the next time step and repeats the process. The optimization is solved again,

taking into account the updated state of the system. This iterative process continues, providing feedback control as the system evolves.

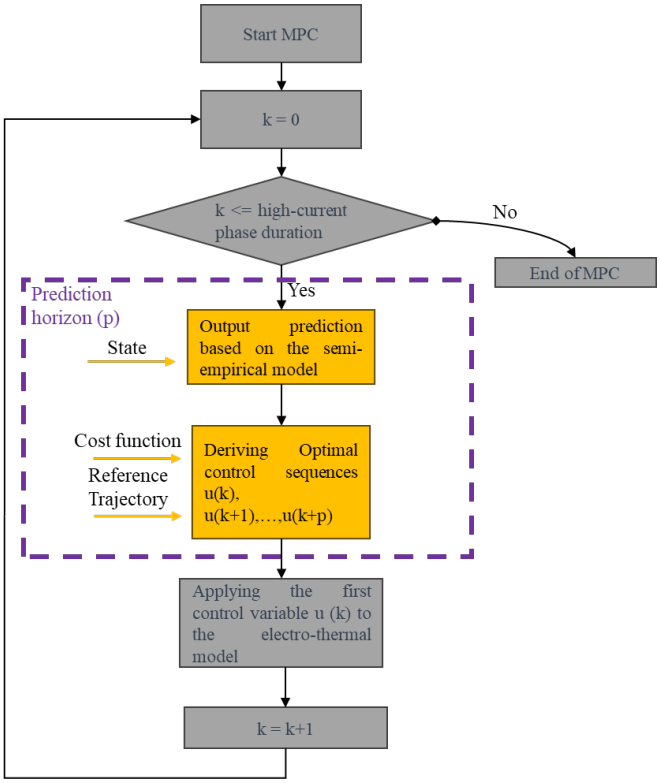

Figure 6. MPC flowchart.

As mentioned earlier, the request for safe and rapid charging strategies has become increasingly crucial, particularly in the context of fast charging [17,25–27]. To address this demand, MPC has emerged as a promising and versatile approach. MPC leverages predictive modelling and real-time optimization to achieve precise control over the charging process.

In this paper, the primary objective of the controller is to concurrently minimize battery temperature while maximizing the SoC. This presents a multifaceted challenge, as the problem entails dealing with a multi-state, constrained, and nonlinear dynamic optimal control scenario. The key states under consideration are the battery temperature (T_{batt}) and SoC, while the control variable at our disposal is the charging current (I_{batt}).

The MPC problem, tailored for fast charging, is defined with strict inequality constraints governing both battery temperature and SoC. By harnessing the probability distribution of estimated battery temperature and SoC levels, MPC strategically determines the charging current rate. The primary objective is to maximize the expected SoC, all while effectively managing and regulating battery temperature within specified limits. This intricate control challenge is encapsulated by a carefully formulated cost function:

$$J = \left[\sum_{k=0}^{N_p-1} \alpha . \frac{1}{SoC(N_p)} + \beta . T_{cell}(N_p) \right] \tag{4}$$

where N_p, representing the prediction horizon, is set to 10 (equivalent to 10 seconds); SoC signifies the charge level at the *k*-th time step; and α and β represent weighting factors. The first component of the cost function is dedicated to maximizing the SoC, aligning with our primary objective. The equality constraint of the MPC is stated as:

$$x(k+1) = f(x(k), u(k)) \tag{5}$$

where $x(k)$ is the state and $u(k)$ is the control input, expressed as follows:

$$x(k) = \begin{bmatrix} T_{cell}(k) \\ SoC(k) \end{bmatrix}, u(k) = [I_{batt}(k)] \tag{6}$$

The inequality constraints are as follows:

$$\begin{pmatrix} T_{cell,min} \leq T_{cell}(k) \leq T_{cell,max} \\ SoC_{min} \leq SoC(k) \leq SoC_{max} \\ I_{batt,min} \leq I_{batt}(k) \leq I_{batt,max} \end{pmatrix} \tag{7}$$

where min and max refer to the minimum and maximum values, respectively.

4.4. Problem Description

This section outlines the study case that forms the basis of our optimization process. Our scenario is rooted in the fast-charging profile detailed in Section 2. For this investigation, we employ an electro-thermal model specifically tailored to the VTC6 3Ah NMC battery.

The control algorithm employed in this study utilizes a receding horizon mechanism. Within this framework, the optimal control sequences within the prediction horizon are computed, and the initial control input is implemented while ensuring compliance with defined constraints. Throughout this study, the constraint values are established as follows:

$$\begin{pmatrix} -20\ °C \leq T_{cell}(k) \leq 45\ °C \\ 0.1 \leq SoC(k) \leq 1 \\ 0 \leq I_{batt}(k) \leq 30 \end{pmatrix} \tag{8}$$

The temperature and current values in use are in accordance with the cell manufacturer's recommendations. Regarding the initial SoC, given that during the initial 0% to 10% SoC range, the cell's temperature is relatively stable, the MPC will focus on optimizing the high-current phase, commencing at 10% SoC. Furthermore, the initial temperature is established at 25 °C, aligning with ambient environmental conditions.

5. Results and Discussion

5.1 Fast-charging Optimization

In Figure 7, the results of the MPC applied during the high-current phase (4C or 12 A) are presented. During this simulation, both weighting factors were set to a value of 1. The optimal outcomes are represented by the red line, while reference values are depicted with a black line.

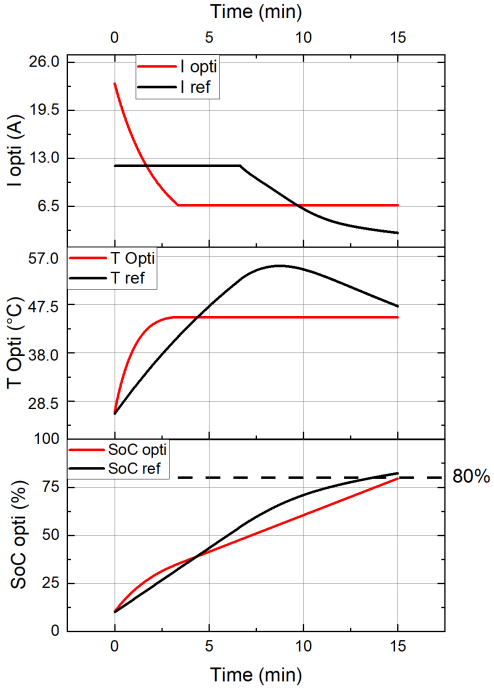

Figure 7. MPC results of the high-current phase.

As observed, the current trajectory computed by the MPC reflects a two-phase charging process. Initially, a high current of 23 A is applied, gradually tapering down to a stable current of

6.5 A. Due to this variation in the current profile, an additional minute is required to reach an 80% SoC compared to the reference profile.

However, it's noteworthy that the optimal charging strategy effectively maintains the cell's temperature below 45 °C, in compliance with the manufacturer's temperature limit, all without the need for an external cooling system. This self-regulation of temperature through the optimal current profile suggests that an undersized cooling system can be employed for this battery pack, potentially resulting in savings in terms of weight, mass, and cost.

The trade-offs observed during the optimization process highlight a delicate balance: while a higher initial current accelerates the SoC increase, it also raises the cell's temperature more rapidly. To prevent overheating, the MPC strategically lowers the current, which slightly extends the charging time but ensures thermal safety. This demonstrates the MPC's effectiveness in achieving a fast-charging profile that optimizes both the SoC and temperature, ultimately enhancing the overall efficiency and safety of the charging process.

5.2. Optimal FC Profile Validation

In this section, the validation of an optimal fast-charging profile was conducted through a rigorous analysis involving both computational modelling and experimental testing. The charging profile, which was derived through an optimization algorithm, was evaluated by comparing the SoC and temperature evolutions. The result of this validation test is shown in Figure 8. These comparisons were made against the results obtained from practical experiments conducted on a VTC6 3A NMC cell.

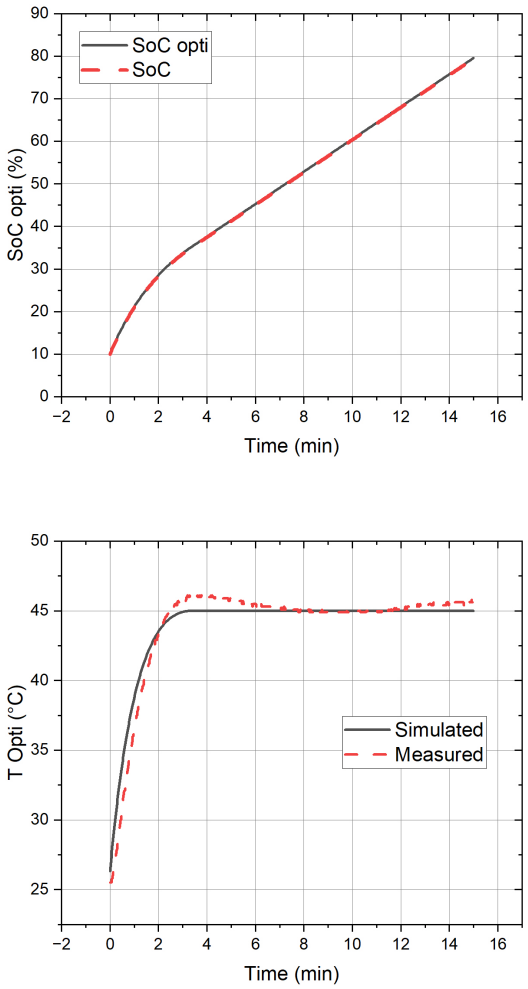

Figure 8. Optimal FC profile validation.

As displayed in Figure 8, the measured SoC and temperature evolution closely match the simulated values. The successful validation of the profile's performance against real-world experimental data demonstrates that the profile not only exists as a theoretical concept simulated by a

simple battery model but underscores the potential for its application in optimizing fast-charging strategies for LiBs, thus it can be applied effectively in practical scenarios.

5.3. Effect of the Current Limit

In the preceding section, the maximum current limit for the MPC was initially set at the manufacturer's recommended maximum C-rate of 10C, equivalent to 30 A. However, considering the specific application, the cells within the battery pack typically operate well below this threshold, not exceeding 4C. Consequently, we conducted a fresh simulation of the MPC using a maximum current limit of 4C (12 A), while maintaining the same weighting factors.

Figure 9 illustrates the results obtained with the 4C current limit. It's evident that the optimal charging profile exhibits a three-phase charging pattern. Initially, a 4C (12 A) charging rate is employed for 3 minutes, followed by a reduction in current to 6.5 A to ensure that the cell's temperature remains below 45 °C. After 15min, the current slowly decreases. While this extended the charging time by more than 1 minute and 30 seconds in comparison to the reference profile, it successfully kept the thermal gradient of the cell within a safe temperature range.

In conclusion, although the temperature remains under the 45 °C limit, it is imperative to conduct a comprehensive lifetime study when utilizing this charging current to evaluate the long-term viability of the optimal charging strategy.

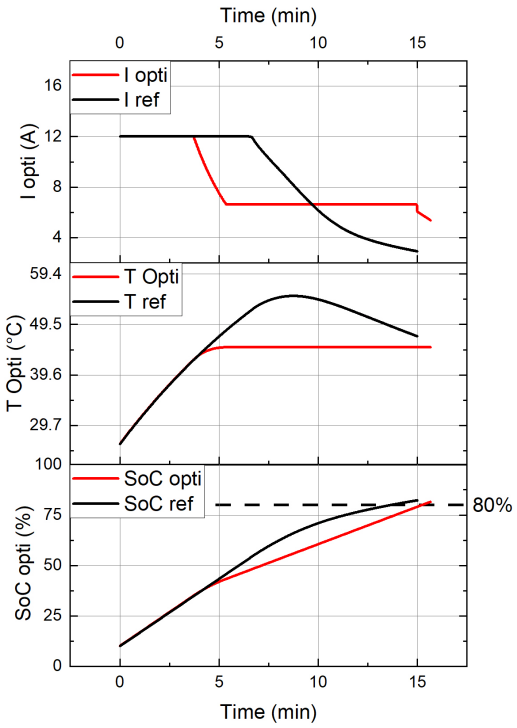

Figure 9. MPC results of the high-current phase using a current limit.

6. Conclusions

In this paper, significant progress has been achieved for optimal fast-charging strategies for LiBs using MPC, with a particular focus on the intricate balance between SoC level and thermal safety. Firstly, the development and rigorous validation of an NMC battery model, employing a single-resistance model framework, showing the accuracy of the simple modelling methodology.

Building upon this groundwork, a tailored MPC system for fast-charging applications has been conceived and implemented. The outcomes reveal an optimal charging profile that not only enhances thermal performance but also entails a minimal trade-off—a mere one-minute extension of the charging duration compared to a typical fast-charging profile.

Significantly, the findings indicate that this optimized charging profile not only facilitates rapid charging but also enables the cell's temperature to self-regulate to the recommended threshold of 45 °C. This development holds the potential to downsize the cooling system, offering substantial cost, weight, and volume savings in battery pack design.

While these achievements are significant, future research endeavours will encompass extending model validation across diverse temperature ranges to ensure robustness under varying environmental conditions. Additionally, a critical task ahead involves the implementation of an exhaustive lifetime study, delving into the long-term implications of the fast-charging strategy on cell durability. Moreover, efforts will be dedicated to enhancing the battery model methodology to further refine with more electrical parameters (e.g., an RC loop). Lastly, the aspiration is to scale up these findings to a broader context, applying them to a battery module, thus aligning our research with the practical demands of real-world applications.

In summary, this work lays the foundation for subsequent explorations into MPC and optimal charging strategies for the development of safer and more efficient fast-charging solutions for Li-ion cells.

Funding

This research received no specific grant from any funding agency in the public, commercial, or not-for-profit sectors.

Data Availability

Data supporting this study are not publicly available due to privacy concerns and the sensitive nature of the information involved.

Acknowledgments

This study is supported by SOLiTHOR BV, Sint-Truiden, Belgium.

Author Contributions

Conceptualization: J.J.; Data curation: J.J.; Formal analysis: J.J.; Funding acquisition: F.B.; Investigation: J.J.; Methodology: J.J.; Project administration: J.J.; Resources: J.J.; Software: J.J.; Supervision: A.D.; Validation: J.J.; Visualization: J.J.; Writing – original draft: J.J.; Writing – review & editing: J.J., & A.D.

Conflicts of Interest

The authors have no conflict of interest to declare.

References

1. Armand, M., Axmann, P., Bresser, D., Copley, M., Edström, K., Ekberg, C., et al. (2020). Lithium-ion batteries–Current state of the art and anticipated developments. *Journal of Power Sources*, *479*, 228708. https://doi.org/10.1016/j.jpowsour.2020.228708
2. Suarez, C., & Martinez, W. (29 September 2019–03 October 2019). *Fast and ultra-fast charging for battery electric vehicles–a review*. 2019 IEEE Energy Conversion Congress and Exposition (ECCE), Baltimore, MD, USA. https://doi.org/10.1109/ECCE.2019.8912594
3. LaMonaca, S., & Ryan, L. (2022). The state of play in electric vehicle charging services–A review of infrastructure provision, players, and policies. *Renewable and Sustainable Energy Reviews*, *154*, 111733. https://doi.org/10.1016/j.rser.2021.111733
4. Liu, S., Liu, X., Dou, R., Zhou, W., Wen, Z., & Liu, L. (2020). Experimental and simulation study on thermal characteristics of 18,650 lithium–iron–phosphate battery with and without spot–welding tabs. *Applied Thermal Engineering*, *166*, 114648. https://doi.org/10.1016/j.applthermaleng.2019.114648
5. Ouyang, D., Weng, J., Chen, M., & Wang, J. (2020). Impact of high-temperature environment on the optimal cycle rate of lithium-ion battery. *Journal of Energy Storage*, *28*, 101242. https://doi.org/10.1016/j.est.2020.101242
6. Zhang, G., Wei, X., Han, G., Dai, H., Zhu, J., Wang, X., et al. (2021). Lithium plating on the anode for lithium-ion batteries during long-term low temperature cycling. *Journal of Power Sources*, *484*, 229312. https://doi.org/10.1016/j.jpowsour.2020.229312
7. Ouyang, D., Weng, J., Chen, M., Wang, J., & Wang, Z. (2022). Electrochemical and thermal characteristics of aging lithium-ion cells after long-term cycling at abusive-temperature environments. *Process Safety and Environmental Protection*, *159*, 1215–1223. https://doi.org/10.1016/j.psep.2022.01.055
8. Inuzuka, S., Shen, T., & Kojima, T. (2020). Dynamic programming based energy management of HEV with three driving modes. In *IOP Conference Series: Materials Science and Engineering* (Vol. 715, No. 1, p. 012063). IOP Publishing. https://doi.org/10.1088/1757-899X/715/1/012063
9. Padovani, T. M., Debert, M., Colin, G., & Chamaillard, Y. (2013). Optimal energy management strategy including battery health through thermal management for hybrid vehicles. *IFAC Proceedings Volumes*, *46*(21), 384–389. https://doi.org/10.3182/20130904-4-JP-2042.00137
10. Park, S., & Ahn, C. (2020). Computationally efficient stochastic model predictive controller for battery thermal management of electric vehicle. *IEEE Transactions on Vehicular Technology*, *69*(8), 8407–8419. https://doi.org/10.1109/TVT.2020.2999939

11. Choi, M. E., Lee, J. S., & Seo, S. W. (2014). Real-time optimization for power management systems of a battery/supercapacitor hybrid energy storage system in electric vehicles. *IEEE Transactions on Vehicular Technology*, *63*(8), 3600–3611. https://doi.org/10.1109/TVT.2014.2305593
12. Zhu, C., Lu, F., Zhang, H., & Mi, C. C. (2018). Robust predictive battery thermal management strategy for connected and automated hybrid electric vehicles based on thermoelectric parameter uncertainty. *IEEE Journal of Emerging and Selected Topics in Power Electronics*, *6*(4), 1796–1805. https://doi.org/10.1109/JESTPE.2018.2852218
13. Afzal, A., Mohammed Samee, A. D., Abdul Razak, R. K., & Ramis, M. K. (2021). Thermal management of modern electric vehicle battery systems (MEVBS). *Journal of Thermal Analysis and Calorimetry*, *144*, 1271–1285. https://doi.org/10.1007/s10973-020-09606-x
14. Zou, C., Manzie, C., & Nešić, D. (2018). Model predictive control for lithium-ion battery optimal charging. *IEEE/ASME Transactions on Mechatronics*, *23*(2), 947–957. https://doi.org/10.1109/TMECH.2018.2798930
15. Zou, C., Hu, X., Wei, Z., Wik, T., & Egardt, B. (2017). Electrochemical estimation and control for lithium-ion battery health-aware fast charging. *IEEE Transactions on Industrial Electronics*, *65*(8), 6635–6645. https://doi.org/10.1109/TIE.2017.2772154
16. Sony. (2015). *Lithium Ion Rechargeable Battery Technical Information*. https://www.kronium.cz/uploads/SONY_US18650VTC6.pdf (accessed 4 September 2024).
17. Berliner, M. D., Jiang, B., Cogswell, D. A., Bazant, M. Z., & Braatz, R. D. (2022). Fast charging of lithium-ion batteries by mathematical reformulation as mixed continuous-discrete simulation. In *2022 American Control Conference (ACC)* (pp. 5265–5270). IEEE. https://doi.org/10.23919/ACC53348.2022.9867170
18. Jaguemont, J., Omar, N., Abdel-Monem, M., Van den Bossche, P., & Van Mierlo, J. (2018). Fast-charging investigation on high-power and high-energy density pouch cells with 3D-thermal model development. *Applied Thermal Engineering*, *128*, 1282–1296. https://doi.org/10.1016/j.applthermaleng.2017.09.068
19. Choe, S. Y., Li, X., & Xiao, M. (2013). Fast charging method based on estimation of ion concentrations using a reduced order of Electrochemical Thermal Model for lithium ion polymer battery. In *2013 World Electric Vehicle Symposium and Exhibition (EVS27)* (pp. 1–11). IEEE. https://doi.org/10.1109/EVS.2013.6914966
20. He, H., Xiong, R., & Fan, J. (2011). Evaluation of lithium-ion battery equivalent circuit models for state of charge estimation by an experimental approach. *Energies*, *4*(4), 582–598. https://doi.org/10.3390/en4040582
21. Jaguemont, J., Boulon, L., & Dubé, Y. (2015). Characterization and modeling of a hybrid-electric-vehicle lithium-ion battery pack at low temperatures. *IEEE Transactions on Vehicular Technology*, *65*(1), 1–14. https://doi.org/10.1109/TVT.2015.2391053
22. White, G., Hales, A., Patel, Y., & Offer, G. (2022). Novel methods for measuring the thermal diffusivity and the thermal conductivity of a lithium-ion battery. *Applied Thermal Engineering*, *212*, 118573. https://doi.org/10.1016/j.applthermaleng.2022.118573
23. Wu, M. S., Liu, K. H., Wang, Y. Y., & Wan, C. C. (2002). Heat dissipation design for lithium-ion batteries. *Journal of Power Sources*, *109*(1), 160–166. https://doi.org/10.1016/S0378-7753(02)00048-4
24. Robinson, P. R., & Cima, D. (2017). Model-Predictive Control Fundamentals. *Springer Handbook of Petroleum Technology*, 833–839. https://doi.org/10.1007/978-3-319-49347-3_26
25. Meng, J., Yue, M., & Diallo, D. (2023). Nonlinear extension of battery constrained predictive charging control with transmission of Jacobian matrix. *International Journal of Electrical Power & Energy Systems*, *146*, 108762. https://doi.org/10.1016/j.ijepes.2022.108762
26. Li, Y., Wik, T., Huang, Y., & Zou, C. (2023). Nonlinear model inversion-based output tracking control for battery fast charging. *IEEE Transactions on Control Systems Technology*, *32*(1), 225–240. https://doi.org/10.1109/TCST.2023.3306240
27. Jia, G., & Cai, X. (2022). Fast charging strategy of lithium-ion batteries with thermal safety margin based on model predictive control. In *2022 41st Chinese Control Conference (CCC)* (pp. 2694–2699). IEEE. https://doi.org/10.23919/CCC55666.2022.9902174